ME Labs
Jack Button: Technical Analyst
Jack Dibachi: Technical Writer
Scott Smith: Team Leader

Experiment 3: Fluid Mechanics

Objectives

The purpose of this report is to show the effects of varying pipe parameters on the major pressure losses downstream of a system of pipes. Secondarily, the objective of this lab is to fully characterize the minor pressure losses of various components of a piping network.

Introduction

Major and minor losses of pressure in piping/plumbing networks are aspects to characterize if said plumbing network is to be fully understood. The most common method of experimentally measuring and determining these pressure losses is to calibrate a differential pressure transducer that can be placed in parallel with any flow. This will result in a minimally invasive way of comparing the pressure difference between any two points in a network. This is a desirable method of measuring pressure, as it minimizes the interference of the sensor in adding loss to the network.

In order to isolate the parameters that affect pressure, a flow sensor must be used to calculate velocity. Assuming that the velocity through identical cross sectional areas of pipe is constant by continuity in incompressible fluids, the velocity should be held constant throughout all lengths of pipe. Thus the flow sensor can be placed anywhere outside the region where pressure drop is being recorded, as long as the inner pipe diameter is known. Two different types of flow meters, which operate in very different ways, can be used to measure the flow rate - and orifice plate, which uses a differential pressure to measure flow rate, and a paddlewheel flowmeter, which uses a turbomachine and an encoder to measure flow rate.

Major and minor losses change with a variety of parameters however, so it is worthwhile to observe the effects of altering these parameters and observe the behavior of the network as it is subject to these changes.

Major losses vary with flow rate/velocity, length, diameter, and friction factor by the following equation:

(Equation 1) $$h_l = f\frac{L}{D}\frac{V^2}{2}$$

Minor losses vary with equivalent length $(\frac{L_e}{D})$ or loss coefficient (K), friction factor, and velocity by the following equation:

(Equation 2) $$h_{lm} = f\frac{L_e}{D}\frac{V^2}{2} \text{ or } h_{lm} = K\frac{V^2}{2}$$

It is important to note that friction factor is a function of the relative roughness of the pipe $\frac{\varepsilon}{D}$, and the Reynolds number R_e, which is a product of density, velocity, pipe diameter, and dynamic viscosity by the following equation:

(Equation 3) $$R_e = \frac{\rho V D}{\mu}$$

As proven in the analysis, the trials in this experiment are exclusively turbulent $(R_e > 2300)$, so the experimental friction factor results can be compared to a Moody diagram or to the Haaland Equation, which is an explicit representation of the Moody diagram governing equation. The Haaland Equation is:

(Equation 4) $$\frac{1}{\sqrt{f}} = -1.8 log\left(\left[\frac{\frac{\varepsilon}{D}}{3.7}\right]^{1.11} + \frac{6.9}{Re}\right)$$

With all of this in mind, and given the material flow properties of water, the friction factor of pipes and the loss coefficient/relative length of minor loss regions can be easily gathered by recording the pressure and flow rate. The result of these calculations is that virtually any network of pipes can be fully characterized using Bernoulli's equation.

(Equation 5) $$\frac{p_2 - p_3}{\rho} + \frac{V_2^2 - V_3^2}{2} + g(z_2 - z_3) = \frac{p_4 - p_5}{\rho} + \frac{V_4^2 - V_5^2}{2} + g(z_4 - z_5) + h_{LA} - h_{LB}$$

Again, by continuity in incompressible fluids:

(Equation 6) $$A_1 V_1 = A_2 V_2$$

Pressure drop can be described at different points of a network through equation 5 (where z_i is the relative height of the point in the pipe).

Methods

The first step of this lab is calibrating the pressure transducer. This can be done very easily by applying various hydrostatic pressures to one side of the transducer (given atmospheric pressure on the other end of the transducer). This hydrostatic pressure is applied through a column of water at known height within a pipe which is connected to one side of the transducer. Hydrostatic pressure is calculated by the following equation:

(Equation 7) $$\Delta p = \rho g h$$

After recording the pressure difference at 5-10 different known heights, a best fit line of input pressure versus output pressure difference readout can be produced and used in further calculations.

Once the pressure transducer has been calibrated, the orifice plate and flowmeter can also be calibrated. All calibration data is listed in Appendix I.

Starting with the paddlewheel flowmeter, the output of the sensor will be a pulse train which can be easily read on an oscilloscope. The frequency of this pulse train is proportionally related to the frequency of the flowmeter. Thus, in order to manually gather the flow rate to relate to this pulse train output, the mass flow rate can be gathered by collecting a mass of water into an empty vessel of known weight and recording the difference of time. The flow rate can be altered by further closing the needle valve to choke flow and reduce flow rate. These values will be related through the following equation:

(Equation 8) $$Q = \frac{\Delta m}{\rho \Delta t}$$

After recording the flow rate at 5-10 different flow rates (again, varied via the needle valve), a best fit curve can be developed which relates the velocity of the flow in the relevant section of the pipe to the pulse train output of the flowmeter. The linear best fit curve show in the Appendix (Fig. 10), has an r-squared value greater than 0.99, thus it was determined that doing a nonlinear fit would be of no use.

Note that, thought the volumetric flow rate isn't immediately valuable or applicable to any previous equations, it is directly used to calculate velocity in the pipes through the following equation:

(Equation 9) $$V = \frac{Q}{A}$$

The orifice plate is calibrated using the pressure transducer and theoretical orifice relations to calculate flow rate. The flow rate through the orifice plate is related to the pressure readout of the transducer by the following equation:

(Equation 10)

$$Q = C_D A_2 \sqrt{\frac{2(P_1 - P_2)}{\rho[1-\beta^4]}},\ \beta = \frac{d}{D}$$

The discharge coefficient C_D follows the relationship shown below, in Figure 1:

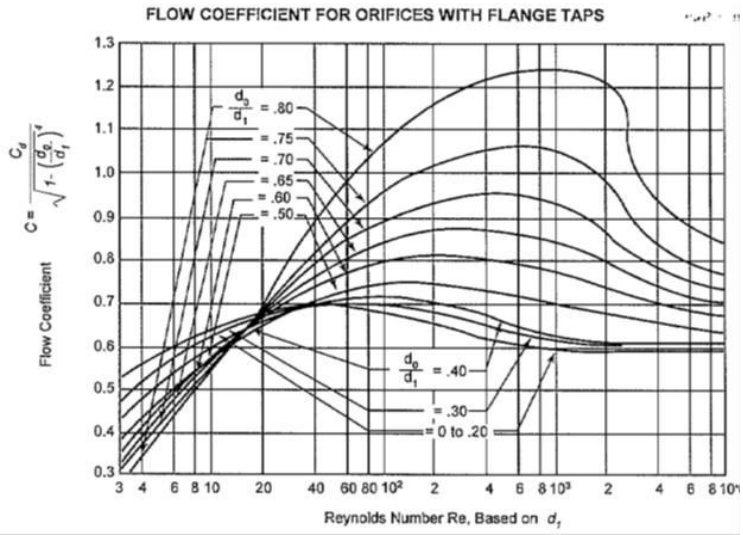

Figure 1: C_D vs. Re

Again, after recording the flow rate at 5-10 different flow rates, a best fit curve can be developed which relates the velocity of the flow in the relevant section of the pipe to the differential pressure reading of the transducer.

Also note that it is critically important to ensure that the pipe length (1-2 ft) just before both the orifice plates and the paddlewheel flowmeter are parallel with the entrance to the sensor. This will ensure that all flow into the sensors is fully developed as each measuring device is highly sensitive to this (as observed in the lab).

All devices have been calibrated, and the calibration data is reported in Appendix I. The next step in the lab is to begin characterizing the pipes by calculating the major pressure losses and further friction factor of pipes of different diameter and at different flow rates.

The first step in doing this is to construct a pipe network which can accomodate 3 pipes, 6 feet long, and a pressure transducer to record the pressure drop across these lengths. Figure 2 displays the way that this setup was achieved.

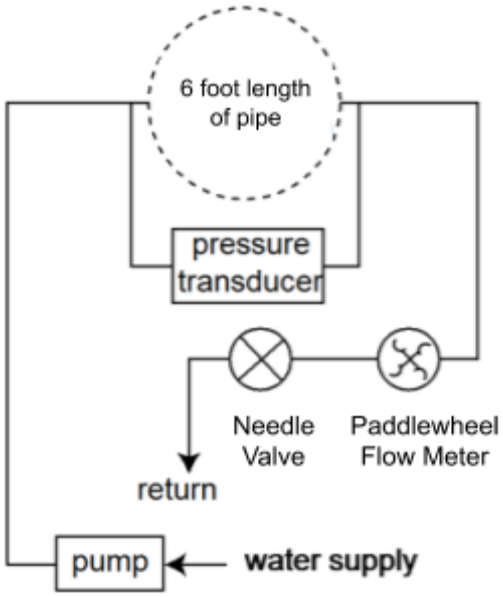

Figure 2: P&ID of the piping network used to characterize the roughness of the lengths of pipe.

Once the network is constructed with the first length of pipe installed, the choke is varied on the needle valve and the flow rate off of the paddlewheel flow meter and the pressure off of the differential transducer at each separate flow rate are recorded. 5-10 different flow rates are selected for recording. This is repeated for each varied diameter length of pipe.

The next step in this lab is to categorize the minor losses in pipe networks. This can be done by constructing three different piping networks of quarter inch diameter to analyze the minor losses through elbows, tees, and couplings. Firstly, the length of pipe should be measured through this variable piping system and volume flow rate measurements should be taken in order to calculate the minor losses. This will allow for the isolation of pressure drop over

minor loss regions and the further calculation of the equivalent length of these regions and/or the loss coefficient of these regions.

Note that measurements should be taken in the turbulent regime in order to allow for consistent friction factor measurements.

Once 5-10 measurements are taken for each type of fitting, the next portion of the lab can begin.

For the wheatstone bridge analysis, an arced tubing segment connected joints 2 and 3 so that the pressure difference between the joints can be recorded with a throttle connected to joint 1 which modifies the flow rate. This is displayed in Figure 3 below.

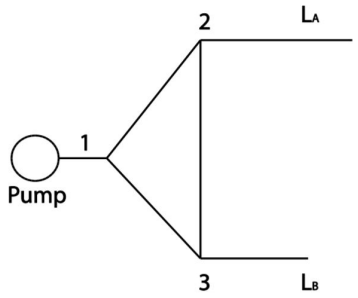

Figure 3: P&ID of the wheatstone bridge constructed for loss observations.

Two 6' long quarter inch diameter tubing should be used as La and Lb. It is important to ensure that these lengths remain straight in order to avoid introducing extra losses. The bead within the arced tube will move in the direction of lowest pressure, indicating lower losses. If, for example, the bead moved to the left then the tubing on the right should be cut shorter until equilibrium is reached.

Next, one end of the pipes should be given a fitting with an associated loss. The change in height required for that length to reach equilibrium will supply the requisite data to calculate the loss coefficient over this fitting. The height difference between the two pipes can be measured so that it can be compared against the accepted minor loss caused by an elbow.

It should be noted that through all experimentation and calibration testing the water temperature was measured with a thermistor to be 20±1°C and was constant through the whole process. This enables us to assume constant thermal water properties in our calculations.

Results

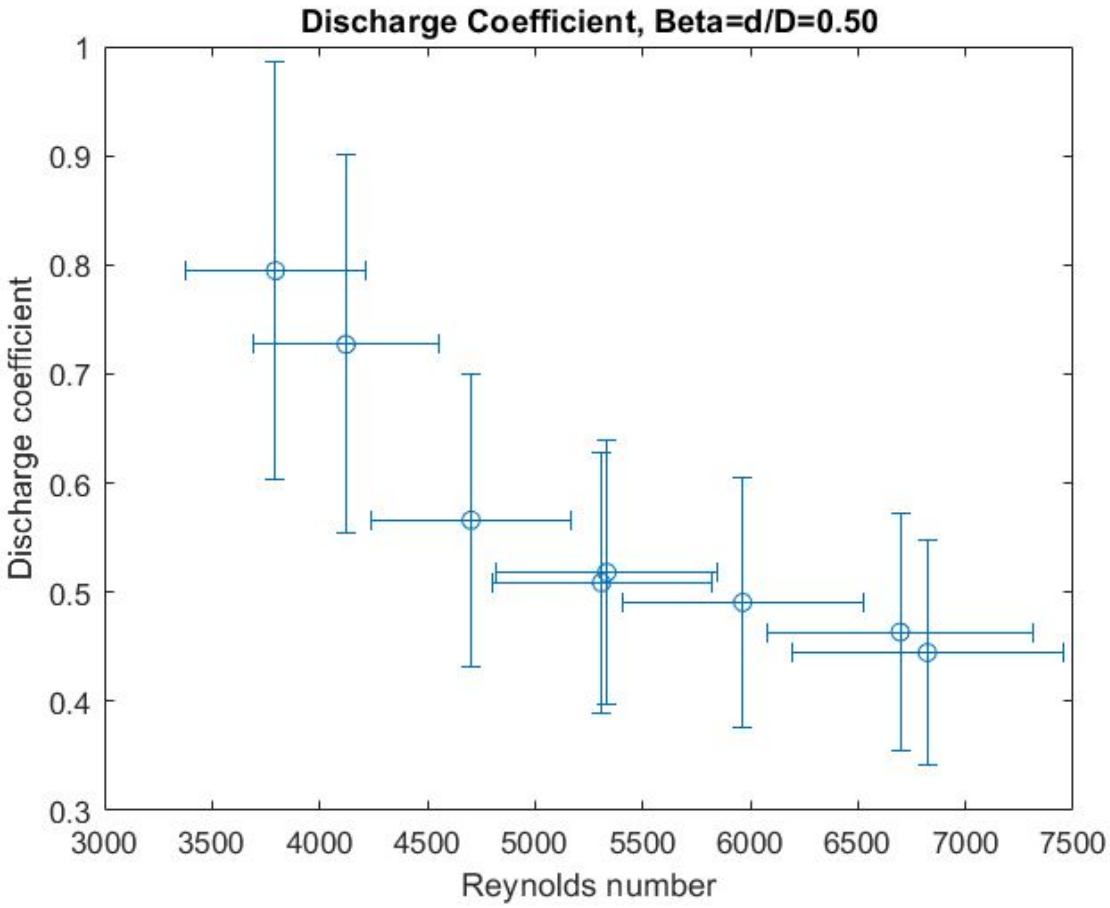

Figure 4: Experimental discharge coefficient vs Reynolds number

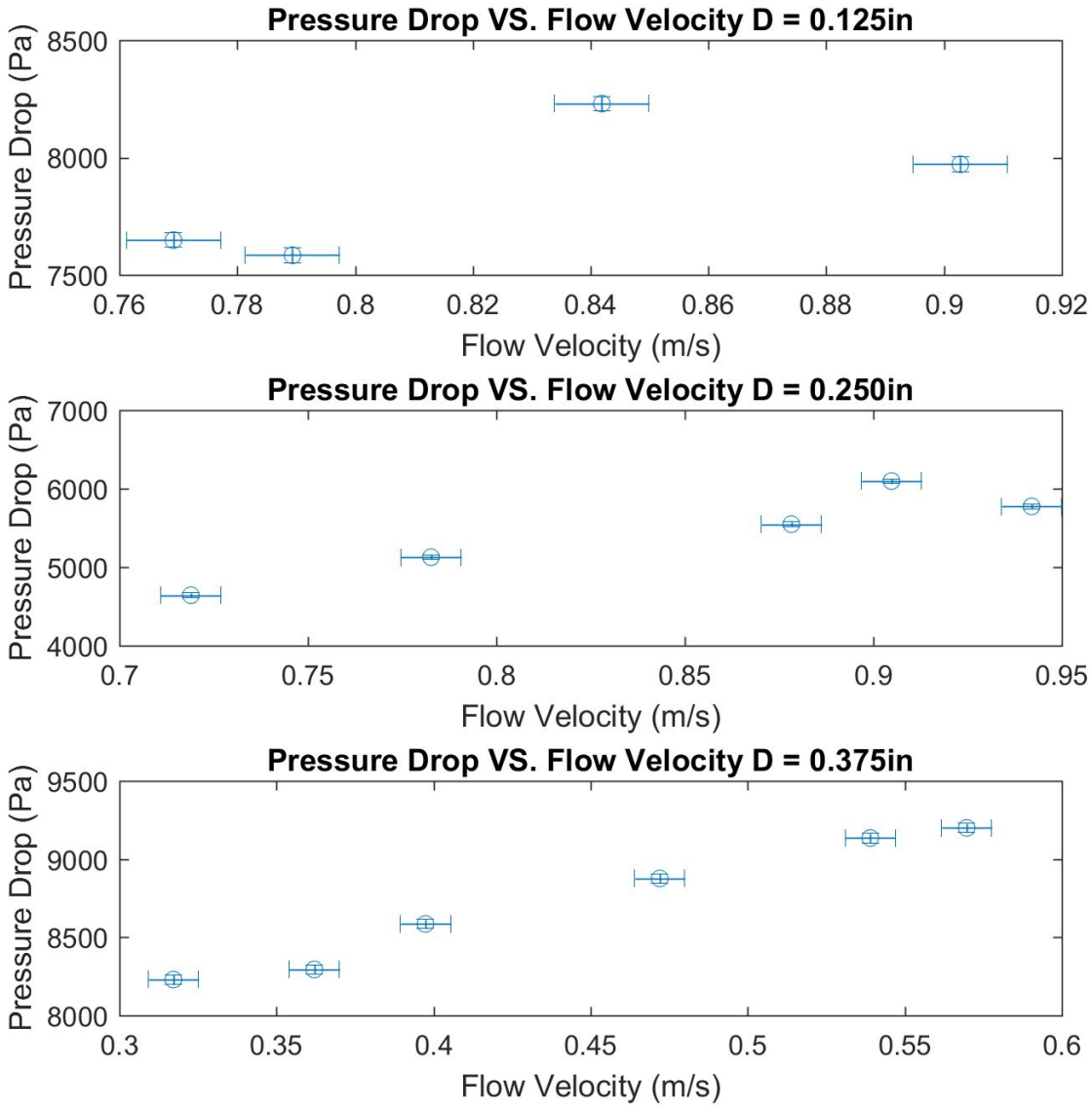

Figure 5: Pressure drop vs. flow velocity over a 1.83 m length of tubing of various diameters.

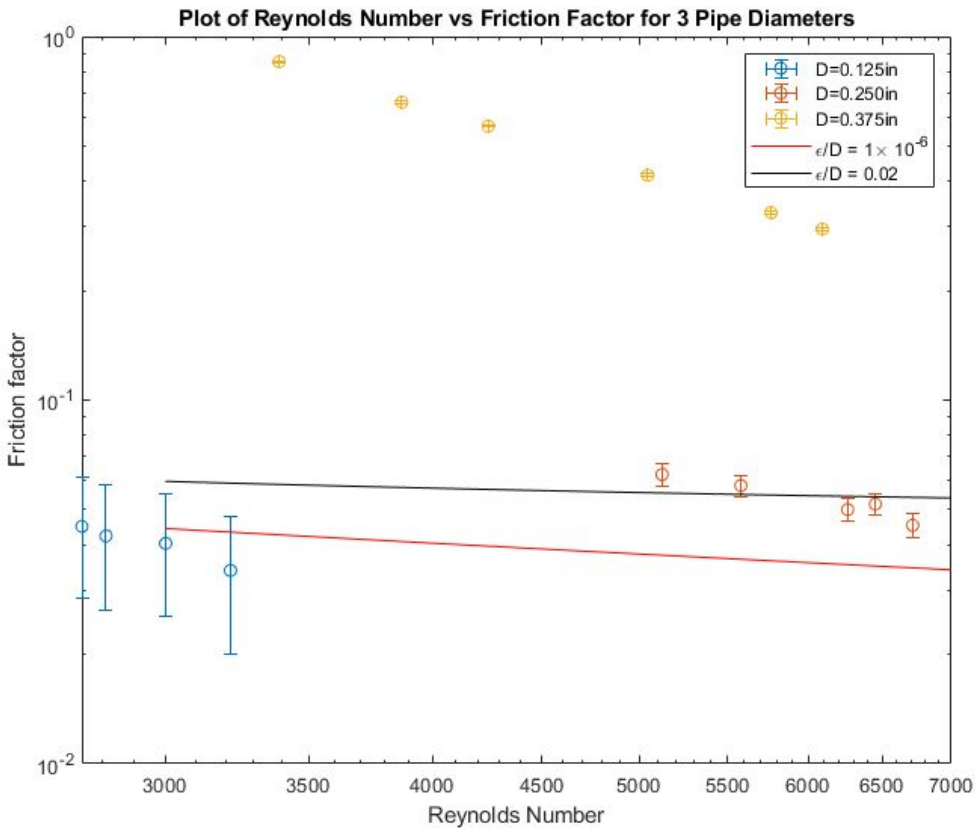

Figure 6: Friction factor vs Reynolds number for the various pipe diameters, compared to Moody Diagram results for different pipe roughnesses.

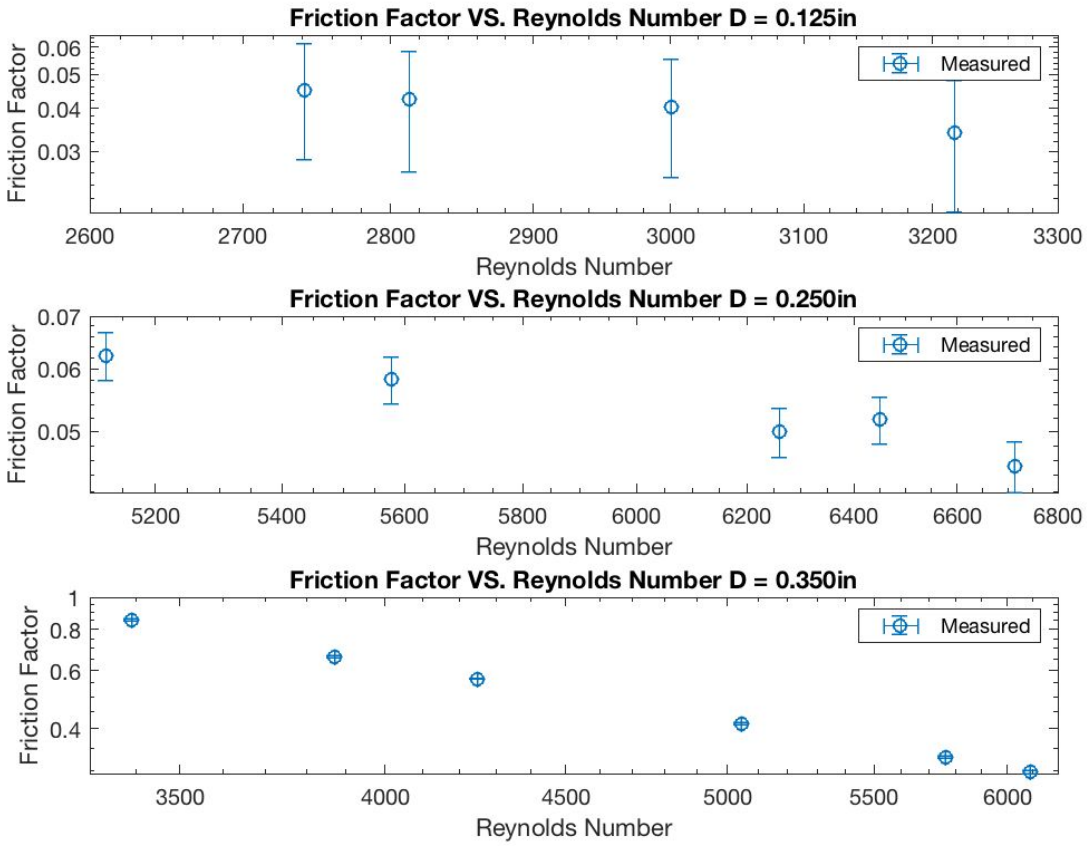

Figure 7: Shows the same data as Figure 6, but isolating each data set.

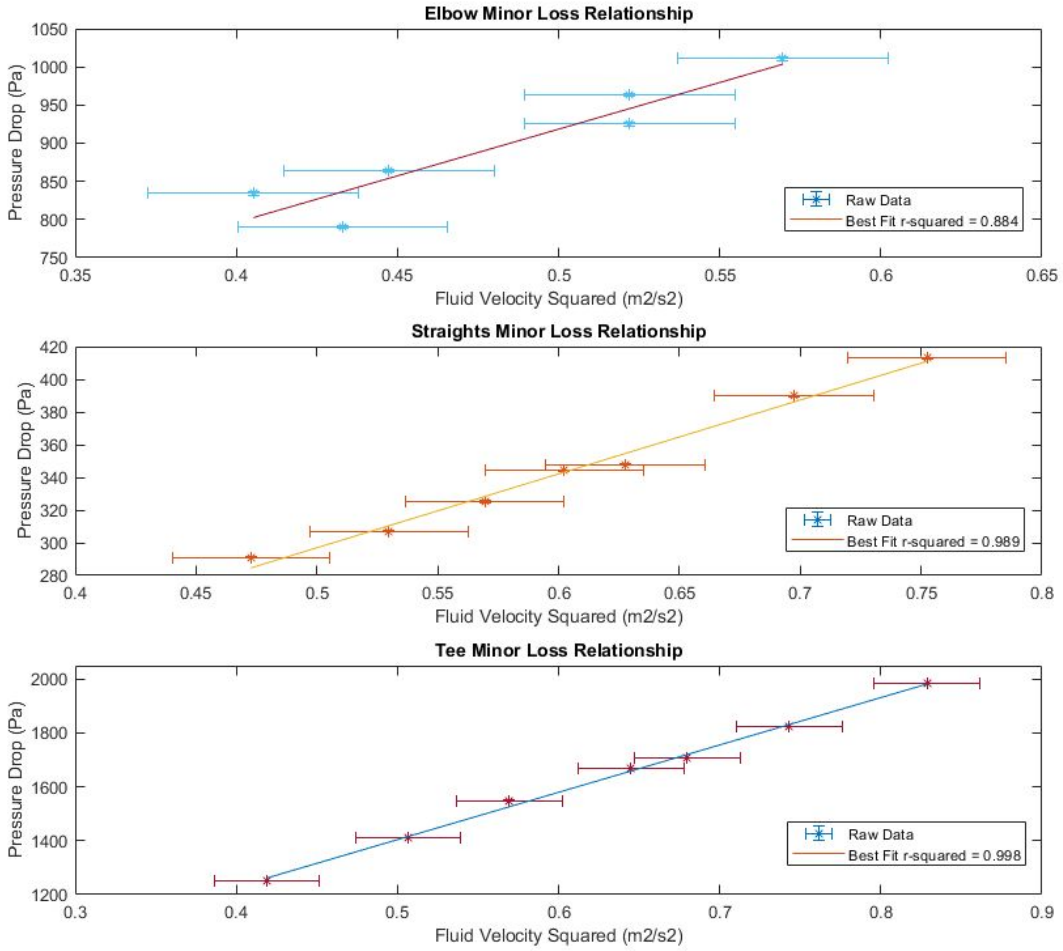

Figure 8: Shows the best fit to the function of minor loss pressure drop VS. fluid velocity squared. The slope of these lines are $\frac{K\rho}{2}$.

Table 1: Minor loss coefficients and equivalent length ratios in various pipe fittings				
Fitting Type	**Experimental K**	**Actual K**	**Experimental Le/D**	**Actual Le/D**
Elbow	0.6 ± 0.1	0.9	40 ± 7	30
Straight Union	0.23 ± 0.01	0.25	15.1 ± 0.7	12
Tee, Straight	0.44 ± 0.02	0.4	15 ± 1	20
Tee, Corner	1.76 ± 0.02	1.8	59 ± 1	60

Table 2: Minor loss for long quarter inch diameter pipe attached to elbow								
Experimental network Le/D	**Initial Pipe Length**	**Length of removed pipe**	**Height Raised till equilibrium**	**Reynolds number**	**Friction Factor**	**Minor Loss**	**Long Tube Le/D**	**Actual Le/D**
40 ± 7	1.8288 ±0.0008 (m)	0.1422± 0.0008 (m)	0.0095 ±0.0008 (m)	4300±500	0.060± 0.005	3.7 ±0.4(m)	34 ±5	30

Discussion

The discharge coefficient changes dramatically with relatively small changes in Reynolds number, dropping almost half within one Reynolds number order of magnitude. In general, the discharge coefficient drops most precipitously in the near-transition region of Reynolds numbers from 3000 to 10000, as depicted in Figure 1. However, the expected range of discharge coefficients for this range of Reynolds numbers is 0.68 to 0.64, while the experimental range of discharge coefficients is 0.79 to 0.45. The uncertainties associated with the plotted data in Figure 4 enclose the expected discharge coefficient values, which means it is possible the orifice plate is behaving as intended, with no unanticipated effects. The discharge coefficient is found by assuming fully developed flow into the entry region of the orifice plate, but boundary layer interference from the entrance pipe fitting could affect the velocity profile before the fluid enters the entry region. Although this effect may not present a significant source of error, it can present a source of uncertainty that is not represented in the data error bars. Although the calibration curve in Figure 8 (Appendix I) has a log slope of 0.79 ± 0.03, indicating a power law relationship with exponent 0.79 ± 0.03, the actual governing equation is a square root relationship, as shown in Equation 10. The discrepancy can be explained by observing how the discharge coefficient changes dramatically, rather than behaving more like a constant. If the discharge coefficient were a constant, or did not vary much, the power law relationship would have an exponent close to 0.5, indicating a square root relationship. However, the discharge coefficient changes dramatically, as shown in Figure 4, so the apparent relation is a power law with an exponent much different than 0.5.

The data is not a reliable means of validating the relationship between friction factor and Reynolds number, as the uncertainty and error intrinsic to the data acquisition methods is too large to obtain results closely resembling those of the Moody Diagram. For example, the pump used for this experiment operates on a cycle which creates a periodically changing pressure and flow rate. While the period of these changes is small, the amplitude is significant enough to

provide widely fluctuating pressures from the transducer console, and a sizeable range of output frequencies from the flowmeter. It is also difficult to keep tubing into the flowmeter and into the length under test perfectly straight without exceeding the counter space of the work station. Thus, it is difficult to determine how tube curvature into the paddlewheel and into the length under test affects the accuracy of the results. Additionally, the order of magnitude of the friction factor determined in the analysis is much different than that of typical drawn tubing. Per the Moody diagram, drawn tubing has a friction factor on the order of 0.00001, whereas the experimental friction factor was 0.05 to 0.06. Although this seems like a dramatic error, inspection of the tubing inner walls reveals long grooves running down the length of the tube, giving a relative pipe roughness much larger than presumably smooth-walled tubing. It is difficult to measure this relative roughness effectively with the tools provided in this experiment, but this undisclosed roughness is likely the source of the discrepancy between the expected friction factor and the experimental friction factor.

Despite some unquantifiable errors in the major loss experiment, the minor loss coefficients and equivalent length ratios for each fitting type were determined within reasonable accuracy, as demonstrated in Table 1. The commonly accepted values for loss coefficient and equivalent length ratio for each fitting are just outside of tolerance for the experimental results, which is likely due to slight bending in the tube lengths between fittings and other unquantifiable errors similar to the ones in the major loss testing.

The equivalent length of the elbow, found using the hydraulic Wheatstone bridge, proved to be reasonably close to that of the general rule of thumb value listed in Table 1. The equivalent length found with the Wheatstone bridge is closer to the accepted value because the arched tube pressure indicator is much more sensitive than the pressure transducer, since it is sensitive to a much smaller range of differences than that of the transducer. Additionally, the sphere inside the tube is tightly fitting, so it is not as sensitive to small, rapid fluctuations in the pressure difference as the transducer is. Thus, a true zero pressure differential is easier to determine with the arched tube than with the pressure transducer, so balancing the loss effects of the branch with the elbow produces much more accurate results than the method using the pressure transducer.

The accuracy of the experimental data, especially the data required to calculate major losses, could be improved by a few changes to the experiment equipment and procedure. For example, using rigid tubing with a known relative roughness would eliminate error due to tube curvature, and would provide a better idea of the expected friction factor for a variety of Reynolds numbers. Additionally, if the flow was driven by a pump with less flow fluctuation, the noise observed from the pressure transducer and the flowmeter would decrease significantly, enabling a better estimate of the true pressure and flow rate values.

Conclusion

The calibration data established linear relationships for the pressure transducer response and the paddlewheel flowmeter response, and a power law relationship for the orifice plate. All the calibrated sensors behaved as expected**,** with the exception of some magnitude differences in the orifice plate discharge coefficient. Although the friction factors in the major loss portion of the experiment were on a reasonable order of magnitude relative to expected values, unquantifiable sources of error like tube curvature, imperfections in tube cutting, and repeatability errors prevented a close fit with the contours of a Moody diagram. With the exception of these unquantifiable errors, minor loss coefficients and equivalent lengths for various pipe fittings were determined with reasonable accuracy when compared with generally accepted values for these types of fittings.

Appendix I: Calibration

Table 1: Orifice Plate calibration data.

Pressure Difference (kPa)	**Volume Flow Rate m^3/s *10^(-3)**
2.46	0.107
4.31	0.163
5.24	0.194
6.71	0.229
7.35	0.235
3.35	0.134
2.24	0.091
4.24	0.164

Figure 8: Orifice calibration data with power fit. R-squared=0.9903

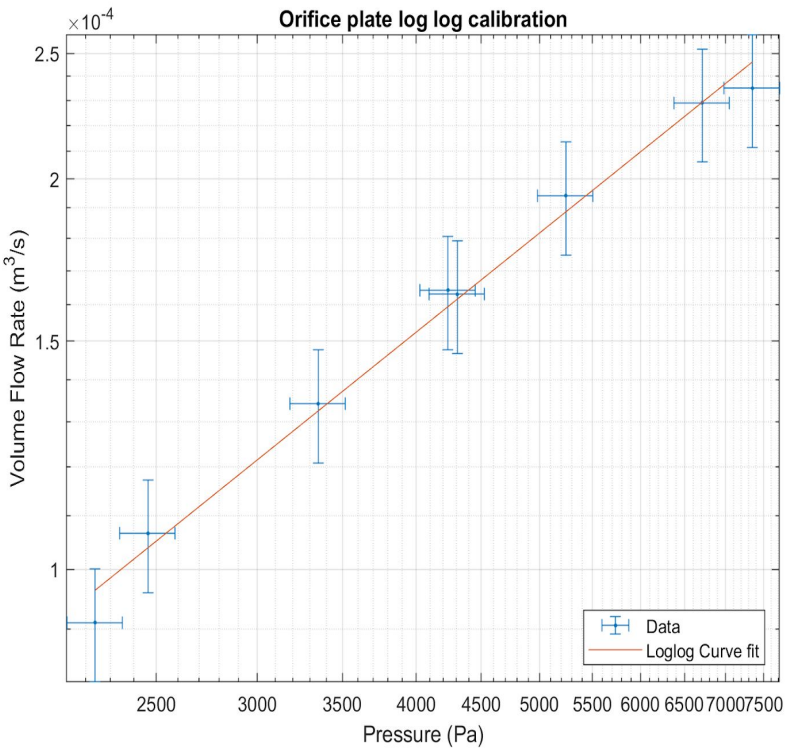

Curve fit data:
Slope = 0.79 ± 0.03 Log(m^3/s)/Log(Pa)

Offset = -6.7 ± 0.2 Log(Pa)

Table 2: Pressure Transducer calibration data.

Pressure Differential (Counts)	Pressure Differential (Pa)*10^4
145.0	1.71
121.0	1.41
96.0	1.11
71.0	0.82
45.0	0.52
32.5	0.37
20.0	0.22
7.0	0.07
0.8	0.0

Figure 9: Pressure Transducer calibration data with linear fit. R-squared=0.9999

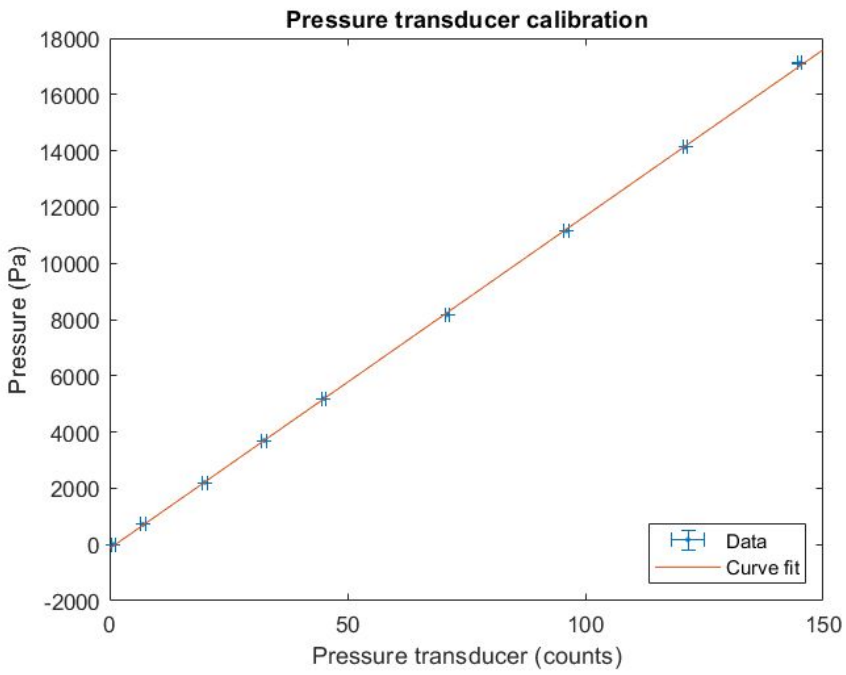

Curve fit data:
Slope = 118.3 ± 0.4 Pa/Count
Offset = -140± 30 Pa

Table 3: Paddlewheel calibration data.	
Paddlewheel Frequency (Hz)	**Volume Flow Rate (m^3/s)*10^-4**
29.3	0.63
24.4	0.54
21.6	0.48
20.4	0.46
17.4	0.42
14.4	0.37
11.7	0.33

Figure 10: Paddlewheel calibration data with linear fit. R-squared=0.9957

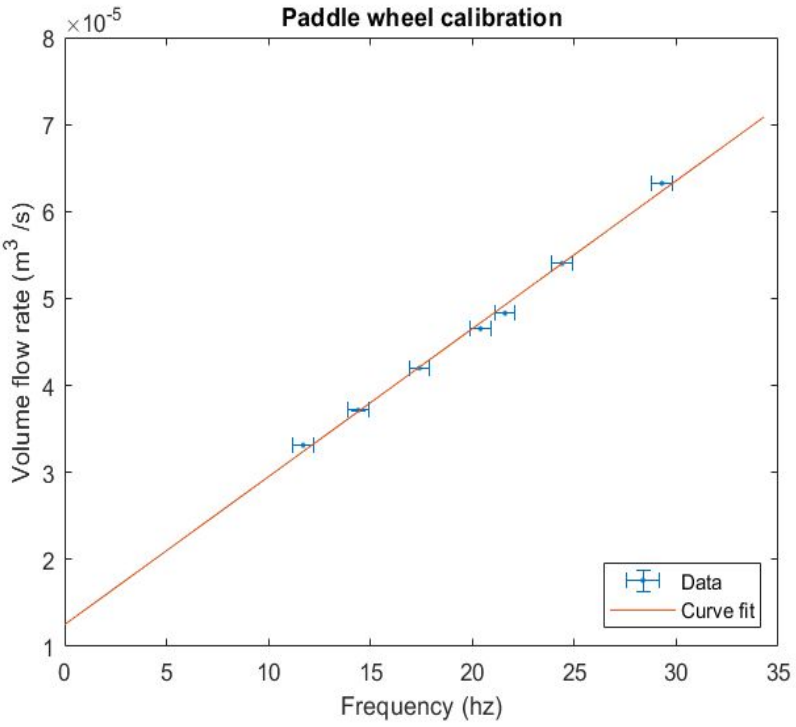

Curve fit data:
Slope = 1.70e-6 ± 5e-8 m^3/s/hz
Offset = 1.2e-5 ± 1e-6 m^3/s

Appendix II: Sources of Uncertainty

There are several sources of uncertainty in this experiment, including pressure transducer uncertainty, oscilloscope uncertainty, stopwatch uncertainty, scale uncertainty, and tape measure uncertainty.

Transducer Uncertainty

From observation during the transducer calibration, the resolution is 0.1 counts, where the counts are the dimensionless value associated with a pressure differential across the transducer. During any dynamic tests, there is significantly more random error due to flow fluctuations from the pump operation, up to ± 1 count.

Oscilloscope Uncertainty

From the oscilloscope documentation on uncertainty, the maximum frequency uncertainty is ± 0.002 Hz, which is negligible compared to the random error due to flow fluctuations imparted on the flowmeter, which is ± 0.5 Hz.

Stopwatch Uncertainty

The stopwatch uncertainty is ± 0.005 s, since the resolution is 0.01 s.

Scale Uncertainty

The uncertainty of the scale used to weigh the water mass is ± 0.5 g.

Tape Measure Uncertainty

The tape measure has a resolution of 0.8 mm, or ± 0.4 mm.

Appendix III: Propagated Uncertainties

Flow Rate

$$\frac{\Delta Q}{Q} = \sqrt{\left(\frac{\Delta \rho}{\rho}\right)^2 + \left(\frac{\Delta m}{m}\right)^2 + \left(\frac{\Delta t}{t}\right)^2}$$

Velocity

$$\frac{\Delta V}{V} = \sqrt{\left(2\frac{\Delta D}{D}\right)^2 + \left(\frac{\Delta Q}{Q}\right)^2}$$

Discharge Coefficient

$$\frac{\Delta C_D}{C_D} = \sqrt{\left(\frac{\Delta Q}{Q}\right)^2 + \left(\frac{1}{2}\frac{\Delta (P_1 - P_2)}{(P_1 - P_2)}\right)^2 + \left(\frac{1}{2}\frac{\Delta \rho}{\rho}\right)^2}$$

Friction Factor

$$\frac{\Delta f}{f} = \sqrt{\left(\frac{\Delta \rho}{\rho}\right)^2 + \left(\frac{\Delta (P_1 - P_2)}{(P_1 - P_2)}\right)^2 + \left(\frac{\Delta D}{D}\right)^2 + \left(\frac{\Delta L}{L}\right)^2 + \left(2\frac{\Delta V}{V}\right)^2}$$

Reynolds Number

$$\frac{\Delta Re}{Re} = \sqrt{\left(\frac{\Delta \rho}{\rho}\right)^2 + \left(\frac{\Delta D}{D}\right)^2 + \left(\frac{\Delta V}{V}\right)^2 + \left(\frac{\Delta \mu}{\mu}\right)^2}$$

Where rho is density, m is mass, t is time, D is diameter, P pressure, L length of tubing, and mu is viscosity.